

Using Two-jet Events to Understand Hadronization

Patrik Edén¹, Gösta Gustafson²
Department of Theoretical Physics
Lund University

Abstract:

While the hard phase of the strong interaction is well described by perturbative QCD, the soft hadronization phase is less understood. Benefiting from the high statistics from e^+e^- experiments at the Z^0 resonance, it is possible to impose strong two-jet cuts on the data without loosing the statistical significance. In these events perturbative activity is suppressed and hadronization effects can be more prominent. We show that after proper event cuts a set of observables are sensitive to differences in the hadronization models. These observables can thus be important tools for a more detailed study of the hadronization mechanism.

¹e-mail patrik@thep.lu.se

²e-mail gosta@thep.lu.se

1 Introduction

High energy reactions like $e^+e^- \rightarrow$ hadrons are usually described in terms of two phases, an initial hard perturbative phase formulated as a parton cascade followed by a soft non-perturbative hadronization phase, for which phenomenological models are needed. The first phase can be calculated from perturbative QCD, but as exact perturbative results in most cases are available only to second order approximate schemes have to be used. In the large N_c limit planar diagrams dominate [1], and for e^+e^- -annihilation, descriptions in terms of parton cascades have been quite successful.

Global features like shape variables (thrust, sphericity, oblateness, major, minor etc.) and inclusive particle spectra in e.g. x_F and p_\perp , reflect mainly the parton distribution in the initial perturbative phase. These observables can be well described assuming that the hadron distribution closely follows the distribution of partons (local parton hadron duality, LPHD [2]), provided a locally invariant cut-off is applied to the cascade. One example is the observed peak position of the distribution in the variable $\xi = \ln(1/x_F)$, which for most hadrons agrees with parton level results, using a virtuality cut-off Q_0 which is larger for heavier hadrons. Also in some more phenomenological models, e.g. in the cluster fragmentation model [3] and the UCLA model [4] the hadronization properties are to a large extent determined by the hadron masses.

A more detailed description of the final hadronic state, including e.g. flavour, the baryon to meson ratio, spin and polarization as well as correlations (including Bose-Einstein correlations), depends also on the non-perturbative properties of QCD, including the structure of the vacuum condensate. These features cannot be obtained from perturbative calculations. Although some of them may in the future be accessible e.g. from lattice calculations, at present it is unavoidable that a model attempting to give a detailed description of the hadronization process must contain a significant number of phenomenological parameters.

To gain insight in the properties of QCD in the soft region and the vacuum structure it is essential to isolate the hadronization process from the perturbative cascade. This is however not an easy problem. At the end of the cascade the running α_s becomes relatively large. The result depends on a necessary infrared cut-off and nonplanar diagrams and interference effects may be important. This implies that this phase is more uncertain and therefore difficult to isolate. It is also possible that the separation between the perturbative and non-perturbative regions cannot be well defined. As discussed in ref [5] a change in the perturbative cut-off can to a large extent be compensated by a modification of the hadronization parameters. The transition region between the two domains may also show interesting coherence effects [6].

In this paper we will study ways to isolate high energy systems with little perturbative activity, in which the non-perturbative features ought to be more prominent. With the very high statistics available from the LEP1 experiments, it is possible to impose event cuts which exclude a significant amount of perturbative activity, and still have remaining events numerous enough for detailed studies of hadronization. It is possible to calculate purity and efficiency measures for different event shape cuts. Our result is however that a simultaneous purity and efficiency close to 1 cannot be obtained; there is no cut that can be called optimal. Instead different cuts are suitable for a study of different features of the hadronization process.

The outline of this paper is as follows: In section 2 we study a set of different event

cuts. In section 3 we study some observables which have been proposed for a separation of different hadronization mechanisms. In section 4 we discuss a few models with different properties and in section 5 their predictions for the considered observables. Conclusions are given in section 6.

Much of the discussion in this paper will concern different aspects of transverse momenta. These will be denoted k_\perp for partons and p_\perp for hadrons. We will also discuss a sum of hadron p_\perp , which we will call Q_\perp .

2 Cuts

We will here discuss a set of event shape cuts suitable to extract events with little perturbative activity. The performance of the cuts are investigated using Monte Carlo simulations, where the underlying parton state is known.

For simulated events we will here with “little perturbative activity” mean events where all gluon emissions occur at a k_\perp below some $k_{\perp 0}$. (In the analysis presented below we will take $k_{\perp 0} = 2$ GeV.) The reason for choosing this definition, rather than e.g. a cut on the sum of E_\perp for all gluons, is that one hard gluon gives rise to a distinct three jet structure, which introduces long range correlations in azimuthal angle. Such a gluon also increases the phase space for softer ones, which enhances its effects on the final state.

Through further emissions, the energy of one gluon is distributed among its emission products. As this rather enhances than reduces the importance of the perturbative phase, we require k_\perp to be smaller than $k_{\perp 0}$ for each emission, and not for the final partons at the end of the cascade.

We examine the performance of the cuts in terms of purity and efficiency. Purity is defined as the rate of events where the highest k_\perp for a gluon emission, $k_{\perp \max}$, is below $k_{\perp 0}$. If the purity is low, perturbative gluons may shadow many hadronization effects. Efficiency is defined as the acceptance rate among the desired events with $k_{\perp \max} < k_{\perp 0}$. If the efficiency is low, the sample might be biased, and the interpretation of the results is more difficult. Low efficiency also implies low statistics.

The cuts are applied to hadronic final states from Z^0 decays, in events generated by the ARIADNE and JETSET MC [7, 8]. ARIADNE is an implementation of the colour dipole formalism for a QCD cascade [9]. This cascade is convenient to use in the present analysis, as it is ordered in k_\perp , which implies that $k_{\perp \max}$ of the cascade is easily extracted as the k_\perp of the first gluon emission. JETSET is a MC for the Lund string fragmentation model [10], which in general gives a good description of e^+e^- data.

The considered two-jet measures are

- $1 - T$ ($T = \text{Thrust} = \max_{\vec{n}_T} \frac{\sum |\vec{n}_T \cdot \vec{p}|}{\sum |p|}$).
- M ($M = \text{Major} = \max_{\vec{n}_M \perp \vec{n}_T} \frac{\sum |\vec{n}_M \cdot \vec{p}|}{\sum |p|}$).
- $k_{\perp \text{clus}}$ = transverse momentum of three-jet configuration found using k_\perp -based cluster method (we have chosen the DICLUS algorithm [11]).
- Sphericity S , which measures the sum of p_\perp^2 w.r.t. the axis minimizing this sum.

- “Linearized sphericity” L , which is similar to sphericity, but linear in particle momenta.
- Multiplicity.

Sphericity S is determined by the largest eigenvalue λ_{\max} to the sphericity tensor

$$S^{\alpha\beta} \equiv \frac{\sum_i p_i^\alpha p_i^\beta}{\sum_i |\mathbf{p}_i|^2}, \quad (1)$$

through the definition $S = \frac{3}{2}(1 - \lambda_{\max})$. Thus $S \approx 0$ for a two-jet event and $S \approx 1$ for an isotropic event. Sphericity is quadratic in particle momenta, which implies that the value is changed if a particle is split in two collinear ones. A linear correspondence to sphericity, suitable for perturbative calculations [12], is obtained by a modified tensor

$$L^{\alpha\beta} \equiv \frac{\sum_i p_i^\alpha p_i^\beta / |\mathbf{p}_i|}{\sum_i |\mathbf{p}_i|}. \quad (2)$$

The quantity $L = \frac{3}{2}(1 - \lambda_{\max}^{(L)})$ thus measures the summed $p_\perp^2/|\mathbf{p}|$ w.r.t. the event axis. In this paper we will use the terminology suggested by Sjöstrand, and call this measure linearized sphericity.

The event shape cuts in thrust, sphericity and jet- k_\perp are widely used to obtain two-jet events. Apart from these quantities, we have chosen to investigate two measures which can be expected to be closely related to the maximal k_\perp of the parton cascade. One is major, which is given by the maximal summed $|\mathbf{p}|$ component orthogonal to the thrust axis, and the other is linearized sphericity discussed above. The cut in multiplicity is used partly to ensure that the more carefully designed cut indeed perform better. Nevertheless it enhances the rate of events with little perturbative activity, as the emitted gluons in general give rise to high multiplicities. One advantage of this cut, which makes it worth consideration, is that p_\perp observables are left relatively unbiased.

Fig 1 shows efficiency and purity results for a $k_{\perp 0} = 2$ GeV for the simulated gluon emissions. Most two-jet cuts perform similarly, but it could be noted that the commonly used cut in $1 - T$ not obviously is the most successful. For large rapidities of the emitted gluon jet, $1 - T$ is approximately $4k_\perp^2/s$ and thus not very restrictive in k_\perp . In the central rapidity region, however, $1 - T$ behaves as k_\perp/\sqrt{s} . For a study in this region, a cut in $1 - T$ therefore performs very similarly to the other ones considered in Fig 1. The multiplicity cut performs noticeably worse than the others. This is expected, since it is not an cut explicitly in a p_\perp variable.

We end this section by noting that the purity and efficiency measures are not very sensitive to the choice of cut. There is thus no optimal cut in all respects, and as we will see, the preferred cut instead depends on the observable under investigation.

3 Observables

In this section we want to study a set of observables which depend on the properties of the hadronization mechanism, but where this dependence is masked by perturbative gluon emission. Thus we will not discuss here the flavour composition of the hadrons, as this

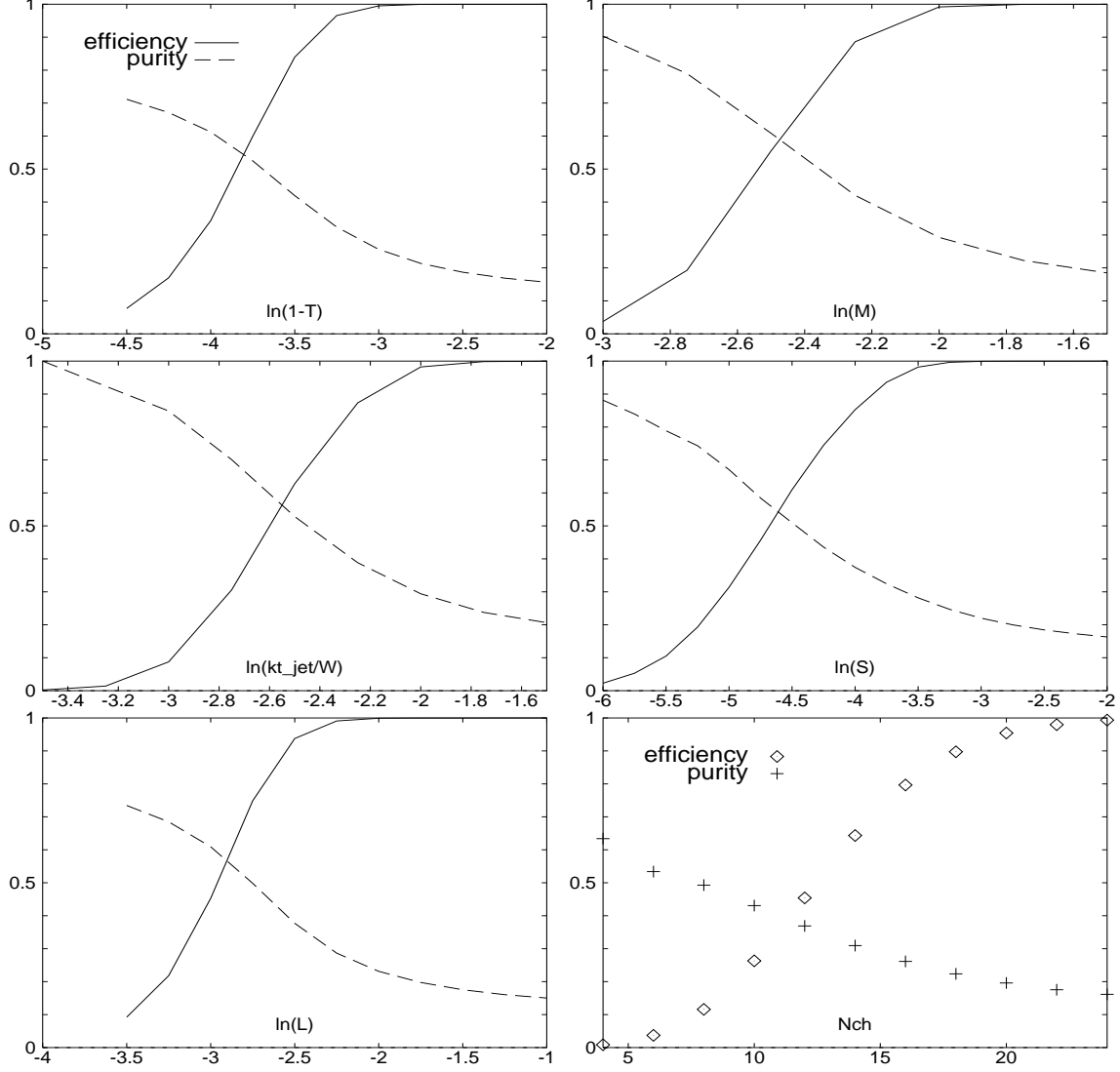


Figure 1: *Purity and efficiency for different two-jet cuts.*

appears to be less affected by gluon radiation. (We note, however, that this may not be completely true, as there are experimental indications for a larger production rate of Λ -particles in Υ decays [13], and also a larger rate of high-energy η -particles in gluon jets [14], than expected from available fragmentation models.)

The observables discussed here are all related to transverse momentum. In many models p_{\perp} of neighbouring hadrons are anti-correlated to a larger or lesser degree. This anti-correlation is counteracted by jet (or minijet) emission, which gives a positive correlation between hadrons close in rapidity, making the analysis of the soft p_{\perp} generation very non-trivial.

3.1 Inclusive p_{\perp} -distribution

The models discussed in the following sections all have tunable parameters for the soft p_{\perp} generation. The values of these parameters can be adjusted to reproduce the inclusive distribution of the hadronic p_{\perp} . Thus this distribution acts as a constraint and cannot be used to separate the different models. For this we have to use more complicated observables, e.g. collective variables or correlations.

3.2 \mathbf{p}_{\perp} transfer

One collective variable which can distinguish between different models is the vector sum $\mathbf{Q}_{\perp}(y)$ of all hadrons with rapidity less than a given rapidity y

$$\mathbf{Q}_{\perp}(y) \equiv \sum_{y_i < y} \mathbf{p}_{\perp i}, \quad (3)$$

which measures the p_{\perp} transfer over the rapidity y . (This variable has frequently been advocated by E. de Wolf [15].) For a longitudinal phase space model constrained by overall momentum conservation, Q_{\perp} grows with the number of particles as a random walk. Thus in this model Q_{\perp} is larger in the central region and larger in events with high multiplicity. In many fragmentation models, however, the \mathbf{p}_{\perp} of a hadron is compensated locally in phase space. In such a model, Q_{\perp} is limited and essentially independent of rapidity and multiplicity.

An essential point when using the Q_{\perp} variable is the choice of axis. In an experiment the direction of the initial $q\bar{q}$ pair is not known. If the thrust axis is used to define the transverse directions, $Q_{\perp}(y)$ is kinematically constrained to be equal to zero for $y = 0$. This definition is therefore very unsuitable, if one wants to use the value of Q_{\perp} in the central region to distinguish between different models.

We have measured Q_{\perp} w.r.t. different axes in MC generated events, using the JETSET default fragmentation scheme, where p_{\perp} is compensated essentially by neighbouring particles in rapidity. This implies that we expect a rapidity plateau in Q_{\perp} , though decays of unstable hadrons and the perturbative activity present in the analysed two-jet events introduce corrections to this result. As seen in Fig 2, both the thrust axis and the linearized sphericity axis by construction create a significant dip in Q_{\perp} when $y = 0$. The sphericity axis, on the other hand, reproduces the plateau extremely well. This should not be over-interpreted, for the reasons mentioned above, but it is clear that the sphericity axis is to prefer in a Q_{\perp} analysis, and it will be used in the results presented below.

The collective quantity Q_{\perp} is sensitive to correlations between neighbouring hadrons. It is also possible to study directly the correlation in p_{\perp} between two hadrons separated by a rapidity interval δy

$$\langle \mathbf{p}_{\perp}(y_1) \cdot \mathbf{p}_{\perp}(y_2 = y_1 + \delta y) \rangle, \quad (4)$$

or the correlation between \mathbf{Q}_{\perp} for two separated y -values

$$\langle \mathbf{Q}_{\perp}(y_1) \cdot \mathbf{Q}_{\perp}(y_2 = y_1 + \delta y) \rangle. \quad (5)$$

The interpretation of these observables will however be hampered by the systematic effects related to the reconstruction of the event axis. In Fig 3 we compare $\langle \mathbf{Q}_{\perp} \cdot \mathbf{Q}_{\perp} \rangle(\delta y)$ for two

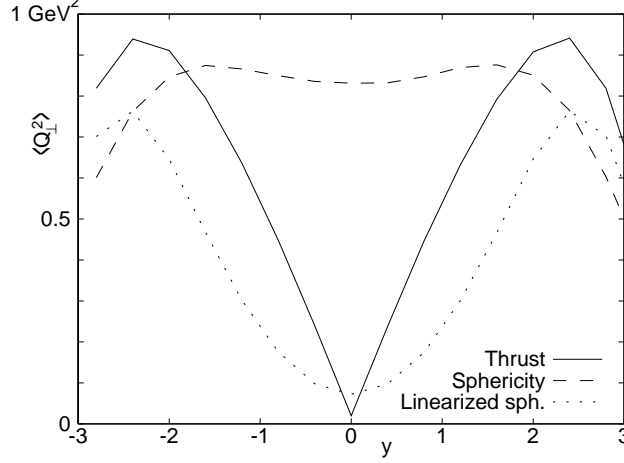


Figure 2: The properties of $\langle Q_{\perp}^2 \rangle$ in MC simulated events depend on the choice of axis. The thrust axis, which maximizes longitudinal momentum, by construction gives $Q_{\perp} = 0$ when $y = 0$. A similar behaviour is seen for Linearized sphericity. The conventional Sphericity axis, minimizing squared transverse momentum, gives the central rapidity plateau expected from the chosen string fragmentation model.

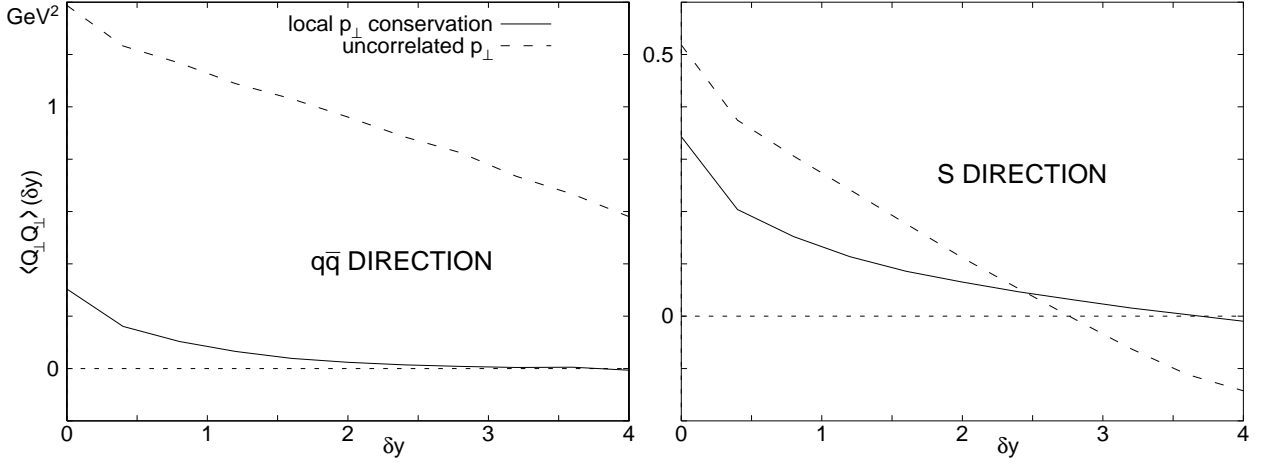


Figure 3: An explicit measurement of the correlation length δy is distorted by the choice of axis. Two very different p_{\perp} compensation models are compared when measured w.r.t. the original $q\bar{q}$ axis (left) and the sphericity axis (right). To emphasize the effects of axis choice, both the parton cascade and hadron decays have been turned off in the simulations.

models, one with local p_{\perp} conservation and one with essentially uncorrelated p_{\perp} . In the MC simulations, we have taken the liberty to turn off both the parton cascade and the hadron decays, in order to more clearly illustrate the effects of axis choice. The plots show the results obtained w.r.t. the original $q\bar{q}$ axis and the sphericity axis, respectively, and it is clear that the behavior of $\langle \mathbf{Q}_{\perp} \cdot \mathbf{Q}_{\perp} \rangle(\delta y)$ is drastically changed. (Equally drastic changes occur if using the thrust axis or linearized sphericity axis.) Due to these effects of axis reconstruction in

e^+e^- , a variation of δy does not seem to provide much more information than is available from the observable $\langle Q_\perp^2 \rangle$. This argument does *not* imply that the δy correlation cannot be an interesting observable in deep inelastic scattering and hadron-hadron collisions, where the event axis is better known.

3.3 Screwiness

A particular correlation between rapidity and azimuthal angle is determined by a variable called screwiness and introduced in ref [6]. Screwiness is defined by

$$S(\omega) \equiv \frac{1}{\langle N(y_{\text{cut}}) \rangle} \left\langle \left| \sum_{|y_i| < y_{\text{cut}}} \exp(i(\omega y_i - \phi_i)) \right|^2 \right\rangle, \quad (6)$$

where y_i and ϕ_i is the rapidity and azimuthal angle for particle i , and the sum runs over all central rapidity particles, specified by some y_{cut} . For large ω the sum describes a random walk along unit vectors in the complex plane, and the absolute square of the sum becomes the average multiplicity in the considered interval, $\langle N(y_{\text{cut}}) \rangle$. We have normalized $S(\omega)$ by this quantity, which implies that it is 1 for large ω .

The screwiness measure is constructed to give a signal for a helix-like correlation between y and ϕ . A motivation why such a correlation might be expected is presented in ref [6] and shortly described in the following section.

4 Models

The most studied hadronization models are based on string dynamics or cluster fragmentation. In the cluster model implemented in the HERWIG MC [16] the gluons split into $q\bar{q}$ pairs at the end of the cascade. A quark is then combined with an adjacent antiquark to form a colourless cluster, which normally decays to two (possibly unstable) hadrons. This approach becomes less realistic and must be modified in events with unusually low gluon radiation. In such events some clusters can get very large masses, and in the HERWIG MC these clusters decay in a stringlike fashion. Consequently, if we select events with low gluon activity we cut away those events for which HERWIG is meant to work best. For this reason we feel that it would not be meaningful to compare such an event sample with HERWIG simulations, and therefore we will instead in the following study some different versions of string hadronization, and for comparison also a model with a p_\perp behaviour similar to a longitudinal phase space.

4.1 String fragmentation

In the Lund string model the confining colour field is assumed to behave as a massless relativistic string starting at a quark, passing the gluons in accordance with their order in colour, and ending at an antiquark. Thus the gluons act as transverse excitations or kinks on the string. The string breaks by the production of $q\bar{q}$ pairs (or occasionally $(qq)(\bar{q}\bar{q})$ systems) which combine to hadrons.

For the longitudinal momentum distribution it is assumed that any breakup divides the string in two causally disconnected pieces, which decay further independently of each other. Together with the assumption of a central rapidity plateau this implies a unique result, the symmetric Lund fragmentation model [17, 10]. The result can be generated in an iterative way with a splitting function of the form

$$f(z) \propto \frac{(1-z)^a}{z} \exp(-bM_\perp^2/z), \quad (7)$$

where M_\perp is the transverse mass of the generated hadron and z is its fraction of jet energy plus longitudinal momentum.

The iterative procedure specifies an ordering of hadrons called rank. The original quark q_0 combines with an antiquark \bar{q}_1 from the $q_1\bar{q}_1$ breakup into the rank one meson. q_1 then forms the rank two meson together with the antiquark \bar{q}_2 from the next breakup, etc. Though the order in rank is not an observable, it is strongly correlated to the order in rapidity.

The string breakup by $q\bar{q}$ creation has been treated as a tunneling process [18, 19], in which the transverse momenta should be described by a Gaussian with a width determined by the string tension κ :

$$\frac{dP}{dk_\perp^2} \propto \exp(-m_\perp^2/\sigma^2). \quad (8)$$

Here $m_\perp^2 = m^2 + k_\perp^2$ is the squared transverse mass of the quark or the antiquark, and from the tunneling mechanism the width should be given by $\sigma^2 = \kappa/\pi$.

An essential property of the string fragmentation is infrared stability, meaning that a soft or collinear gluon has only little influence on the string motion and therefore also on the final hadronic state³. This feature makes the result less sensitive to the cutoff for the partonic cascade, and a change in the cutoff can be well compensated by a change in the hadronization parameters when looking at event shapes and inclusive observables for the total event sample [5]. Thus a larger cutoff is compensated by a larger width σ for the hadronization k_\perp . Some differences may remain, however, as a gluon tends to give extra k_\perp in the same direction to neighbouring hadrons, while hadronization- p_\perp tends to be in opposite directions, depending on the details in the fragmentation model.

In section 3.2 we discussed an observable called \mathbf{Q}_\perp , which is sensitive to the properties of p_\perp compensation. We will continue this section by describing different hadronization- p_\perp models, which give slightly different predictions on Q_\perp and the other observables discussed in section 3. In section 5 we examine how well these differences can be distinguished in a two-jet event sample.

4.2 JETSET default

In the JETSET default version of the string fragmentation model the $q\bar{q}$ breakups of the string are uncorrelated both in transverse momentum and in flavour. As the quark and the antiquark in a pair have balancing k_\perp the transverse momentum of one hadron is fully

³To treat situations where a hadron obtains energy and momentum from several small string pieces is however not uniquely specified from the string dynamics. In the models studied below we will use the method developed by Sjöstrand [20] and implemented in the JETSET MC.

compensated by its two neighbours in rank. This implies that p_\perp is conserved very locally in rapidity.

From Eq (8) we expect that the width of the k_\perp -distribution should be given by $\sqrt{\kappa/\pi} \approx 250$ MeV, but in applications it is treated as a tunable parameter, correlated to the cut-off for the parton cascade. Fits to data give a value around 360 to 400 MeV. Eq (8) also introduces an overall suppression of heavy quarks. This implies that the rate of c is completely negligible (the c/u ratio is $\sim 10^{-11}$). To get the rate of s -quarks we would have to know its effective mass. The observed s/u ratio around 1/3 corresponds to the very reasonable value 250 MeV.

Studies of photons at LEP1 indicate a larger tail for high- p_\perp π^0 s [21]. The origin of this tail is not clear, but in JETSET default a small component with higher p_\perp is included (k_\perp is multiplied by a factor of 2 for 1% of the vertices).

4.3 Partial p_\perp Compensation

The production rate for η and η' cannot be reproduced if neighbouring string breakups are uncorrelated in flavour. Also studies of two-particle correlations observed in hadron–hadron collisions are not well described if the \mathbf{k}_\perp in different breakups are totally uncorrelated [22]. As discussed above, this would imply that the p_\perp of a hadron is fully compensated by its two neighbours in rank. In ref [23] a model is presented in which there are correlations in flavour and k_\perp with some finite correlation length. The model implies a suppression of η and η' production, and also that only a fraction $\gamma < 1$ of the p_\perp of a hadron is compensated by the neighbouring hadrons in rank. Thus p_\perp is compensated within a finite correlation length, but this range is larger than in JETSET default.

In [23] it is shown that this p_\perp compensation assumption can be embedded in an iterative fragmentation scheme. The inclusive p_\perp distribution is then a Gaussian,

$$dP \propto \exp\left(-\frac{\alpha}{2\gamma}p_\perp^2\right)d^2\mathbf{p}_\perp, \quad (9)$$

where α is a tunable parameter. Furthermore, the sum in \mathbf{p}_\perp for the first i particles in rank, $\mathbf{Q}_{\perp i}$, saturates for large i towards the distribution

$$dP \propto \exp(-\alpha Q_\perp^2)d^2\mathbf{Q}_\perp. \quad (10)$$

We note that for fixed $\langle p_\perp^2 \rangle$ for the hadrons, the collective variable $\langle Q_{\perp i}^2 \rangle$ is smaller for larger γ . This is just the previously stated behaviour for the closely related observable $\langle Q_\perp^2(y) \rangle$, which is small if p_\perp is conserved locally in rapidity.

The JETSET default algorithm is retrieved by setting $\gamma = 1$ and $\alpha = 1/\sigma^2$, where σ is the width in Eq (8). In [23], γ is instead assumed to depend on the hadron mass M , and is parametrized as

$$\gamma = \frac{1}{1 + M_0/M}, \quad (11)$$

where M_0 is set to 0.9 GeV.

4.4 Uncorrelated p_\perp

To test whether the data really show a local p_\perp conservation, we also want to study a situation where the hadronic transverse momenta are uncorrelated apart from overall p_\perp

conservation. This can be achieved by pushing M_0 to infinity in Eq (11), which corresponds to γ being small, but keeping α/γ finite. The MC from [23] is not designed to cope with very large M_0 -values. When hadrons are peeled off from both ends of the string usually a large p_\perp is built up for a remaining string piece in the centre. Such events have to be discarded, keeping only those events where by chance this string piece has limited p_\perp . In this paper we study only central particles in the accepted events, and thus for our purposes we obtain a fair estimate of the result if in the MC we peel off hadrons from one end only, pushing the junction to the other and outside the region of study.

4.5 The UCLA model

A partial p_\perp compensation is also assumed in the UCLA model [4]. In this model it is assumed that not only the longitudinal momentum distribution but also the flavour composition and the distribution in transverse momentum are determined by the symmetric fragmentation function in Eq (7). Thus in this model the quark degrees of freedom do not appear explicitly, but only the momenta and flavour of the hadrons. A direct application of Eq (7) will however give a too wide p_\perp -distribution. In the UCLA approach this problem is solved by assuming a similar kind of finite p_\perp correlations as in the model in section 4.3, with $\gamma = 1/2$. Thus as far as transverse momentum goes we expect rather similar results for the UCLA model and the model in [23], and for this reason we content ourselves to study the latter in our investigations.

4.6 Helix String

At the end of a perturbative parton cascade the virtualities become relatively small and the running coupling therefore relatively large. This implies that interference and coherence effects are expected to be important. In ref [6] arguments are presented for correlations between rapidity and azimuthal angle for the emitted gluons, which correspond to a helix-like field at the end of the cascade. This field configuration has also some similarities with a string coupled to a gauge field or a massive relativistic string [24].

A modification to the Lund fragmentation scheme reflecting the helix-like field is presented in [6]. The rapidity distance Δy between two string breakups is correlated with the azimuthal angle $\Delta\phi$ between the transverse direction of the two produced $q\bar{q}$ pairs. The pitch of the helix is given by an unknown parameter $\Delta y/\Delta\phi = \tau$, allowing for some Gaussian fluctuations around this value. This implies that the observable $S(\omega)$ defined in section 3.3 gets a peak at $\omega \approx 1/\tau$. Expected values of τ are around 0.3 to 0.5. The string energy per unit rapidity available to generate p_\perp is given by a parameter m , which implies that a typical magnitude of hadron p_\perp is given by $m\tau$.

4.7 Time Dependent p_\perp

In order to investigate the sensitivity of the observables we will also study a model with a correlation between transverse momentum and multiplicity which might not be totally inconceivable. The results in Eq (8) with a constant width corresponds to a situation with a static flux tube or stringlike colour field. The estimated width of this flux tube is of the

order of 1 fm. One can imagine that at very early times the flux is more concentrated. This might correspond to a larger effective string tension, and also from the uncertainty relation one might then imagine that larger transverse momenta are produced in early breakups. If the transverse dimension of the flux tube equals the proper time τ , then we could expect fluctuations in k_\perp of the order $2/\tau$. Expressed in the variable $\Gamma = \kappa^2 \tau^2$ this corresponds to a width $\sigma^2 \sim 4\kappa^2/\Gamma$. This becomes very large when $\Gamma \rightarrow 0$, and from a string picture we should expect a saturation. To produce large k_\perp sufficient energy must be stored in the string, which therefore must have a minimum length. As discussed in [19] we expect a suppression when $k_\perp > \kappa\tau$, and thus a saturation when $2/\tau \sim \kappa\tau$ or $\Gamma \sim 2\kappa$. These arguments would give the following width for the k_\perp -generation

$$\sigma^2 = \begin{cases} \frac{\kappa}{\pi} + \frac{4\kappa^2}{\Gamma}, & \Gamma < 2\kappa \\ \sigma_{\max}^2 = \frac{\kappa}{\pi} + 2\kappa, & \Gamma > 2\kappa \end{cases} \quad (12)$$

Actually this expression does reproduce the inclusive p_\perp spectrum with hardly any tuning. In our calculations we allowed for an overall normalization factor on σ ,

$$\sigma \rightarrow \chi\sigma. \quad (13)$$

For the standard perturbative cutoff we get $\chi = 1.08$.

A special consequence of the time dependent k_\perp width is a strong correlation between transverse momentum and multiplicity. An early breakup splits the original system in two pieces with relatively small invariant masses. If these masses are called M_1 and M_2 we have approximately

$$M_1^2 M_2^2 \approx \Gamma s, \quad (14)$$

where \sqrt{s} is the total mass of the system. It is also easy to show that the ensuing depletion in multiplicity appears in a rapidity of size $\Delta y \sim \ln(\langle \Gamma \rangle / \Gamma)$ around the breakup, where $\langle \Gamma \rangle$ denotes the average value of Γ .

5 Results

5.1 Hadron p_\perp spectra

We have used average p_\perp and average multiplicity to impose constraints on the free parameters of the considered models. For simplicity, we have left the ARIADNE+JETSET default algorithm unchanged and tuned the other models to reproduce its values. Differences are then searched for in other observables, which will be discussed below.

All models depend on the $k_{\perp\text{cut}}$ of the cascade and the a and b parameters of the symmetric fragmentation function Eq (7). To compare different hadronization models, we are interested in using the same description of the perturbative phase for all models, and we have therefore tuned all models keeping the cascade cut-off $k_{\perp\text{cut}}$ constant to the ARIADNE default value. As $k_{\perp\text{cut}}$ is also an hadronization parameter, we will in some examples compare tunes of the same model with different values of $k_{\perp\text{cut}}$.

The a and b parameters influence the multiplicity distribution. For each setup of other parameters, there is in general a narrow but long band of values in the a and b parameter

model	parameters			others			$\langle N \rangle$	$\langle p_{\perp} \rangle$
	$k_{\perp \text{cut}}$ (GeV)	a	b (GeV ⁻²)					
Default				$\sigma_{k_{\perp}}$ (GeV)				
	0.6	0.23	0.34	0.405			34.9	0.60
	1.5	0.5	0.4	0.42			35.1	0.59
Partial p_{\perp}				$\frac{1}{\sqrt{\alpha}}$ (GeV)	M_0 (GeV)			
Compens.	0.6	0.23	0.34	0.67	0.9		34.9	0.60
Uncorr. p_{\perp}	0.6	0.23	0.34	1.52	10		34.8	0.59
Helix				τ	σ_{τ}	m (GeV)		
	0.6	0.23	0.37	0.3	0.2	1.1	35.0	0.59
	0.6	0.23	0.39	0.5	0.3	0.8	34.8	0.60
	0.6	0.23	0.4	0.7	0.35	0.68	34.6	0.60
Time Dep. p_{\perp}				χ				
	0.6	0.23	0.34	1.08			34.7	0.60
	1.5	0.5	0.42	1.18			34.7	0.60

Table 1: *The tuned parameter values of the considered models. The tunes are performed w.r.t. average multiplicity $\langle N \rangle$, with π^0 stable, and average $\langle p_{\perp} \rangle$ within a rapidity interval $|y| < y_{\text{cut}} = 3$. $\langle p_{\perp} \rangle$ is measured w.r.t. thrust axis and defined as $\frac{1}{n_{\text{ev}} \langle N(y_{\text{cut}}) \rangle} \sum_{\text{ev}} \sum_{|y| < y_{\text{cut}}} |p_{\perp}|$. The top line of the models is the ARIADNE+JETSET default tune which has not been changed. The other models are tuned to give similar results. The models and their parameters are discussed in section 4.*

space which reproduces the average multiplicity. The specific a and b values in the tunes are chosen to give a fair agreement also on multiplicity dispersion. The result is presented in Table 1.

p_{\perp} in low multiplicity events

The different models have been tuned to give similar p_{\perp} distributions in the full event sample. After a two-jet cut, the p_{\perp} distribution may differ, as the importance of the perturbative phase is then reduced. We will here investigate that possibility. Among the two-jet cuts discussed in section 2, the rather blunt cut in multiplicity is then of interest, as it introduces little bias to the p_{\perp} spectrum.

In section 4.7, we discussed a model where the proper time of a $q\bar{q}$ vertex in the string influences the width of the k_{\perp} distribution for the $q\bar{q}$ pair. This model introduces correlations between average p_{\perp} and multiplicity.

Gluon emissions in general contribute both to p_{\perp} and multiplicity. For soft gluons the effects are smaller, but if their contribution to p_{\perp} dominates, it affects the average p_{\perp} in low-multiplicity events. Thus it is of interest to compare correlations in $\langle p_{\perp} \rangle$ and multiplicity for the same fragmentation model tuned with different cascade cutoffs.

In Fig 4 we compare the time dependent p_{\perp} model discussed in section 4.7 and JETSET default fragmentation by studying average p_{\perp} of particles in the central rapidity region

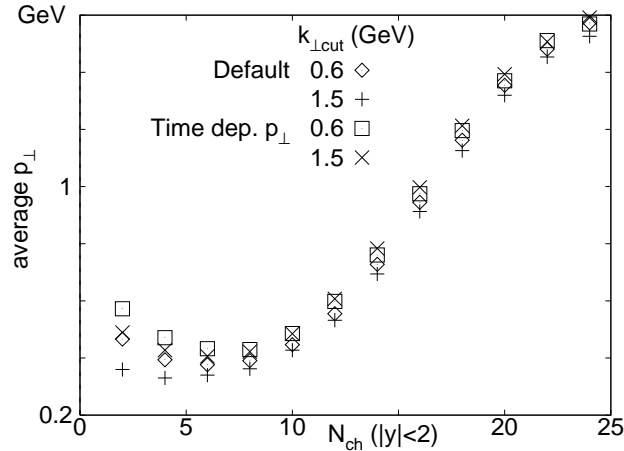


Figure 4: Average p_{\perp} w.r.t. thrust axis for different charged multiplicities. Statistical errors are well within symbol sizes. The correlation between p_{\perp} and multiplicity in the time dependent p_{\perp} model is seen as a higher prediction for average p_{\perp} in low multiplicity events. For both models $\langle p_{\perp} \rangle$ is higher in low multiplicity events when the cascade cutoff $k_{\perp\text{cut}}$ is lowered. This indicates that soft gluons in these models give a larger contribution to hadron p_{\perp} than to hadron multiplicities.

$|y| < 2$, as a function of the charged multiplicity N_{ch} in that region. As expected, average p_{\perp} at low multiplicities is larger in the time dependent p_{\perp} model. p_{\perp} and y are defined w.r.t. the thrust axis, and no two-jet cut in a p_{\perp} measure is imposed on the event sample.

We note that $\langle p_{\perp} \rangle$ at low multiplicities is higher for both models if the cascade cutoff is reduced from 1.5 GeV to 0.6 GeV. In the dipole cascade combined with string fragmentation, the soft gluons in this range of k_{\perp} thus contributes to hadron p_{\perp} more than to hadron multiplicities.

We have also checked the prediction for the time dependent p_{\perp} model if the expected saturation of the $q\bar{q}$ k_{\perp} width at very early breakups is neglected. We then get a significantly higher prediction for $\langle p_{\perp} \rangle$. When $N_{\text{ch}}(|y| < 2) = 2$, it lies between 0.9 and 1.2 GeV, depending on the $k_{\perp\text{cut}}$ for the cascade. The correlation in p_{\perp} and multiplicity is thus and observable which can be used to confront this kind of unexpected p_{\perp} generation with experimental data.

5.2 p_{\perp} transfer

The observable $Q_{\perp}(y)$ discussed in section 3.2 measures the p_{\perp} transfer over the rapidity y and is sensitive to correlations in hadron p_{\perp} . We have investigated Q_{\perp} for different assumptions about hadron p_{\perp} conservation. In the default algorithm, p_{\perp} is compensated by the neighbours in rank, which implies a compensation local in rapidity. In the partial p_{\perp} compensation model, a fraction $\gamma < 1$ of p_{\perp} is compensated by closest neighbours. This implies a correlation length for p_{\perp} of order $1/\gamma$ which is finite, but larger than for JETSET default. We also examine a model where the hadron p_{\perp} are uncorrelated, apart from global momentum conservation.

$\langle Q_{\perp}^2 \rangle (\text{GeV}^2)$	default		partial p_{\perp} compens.	uncorr. p_{\perp}
$k_{\perp\text{cut}} (\text{GeV})$	1.5	0.6	0.6	0.6
No cascade	-	0.60	0.71	0.74
With cascade, all events	12.2	12.3	12.4	12.6
two-jet events	0.86	0.94	1.02	1.09

Table 2: Average Q_{\perp}^2 , measured w.r.t. the sphericity axis in a central rapidity range $|y| < 2$. Results for different assumptions about hadron p_{\perp} correlation lengts. The differences in the predictions are shadowed by the perturbative cascade, but can be restored by a two-jet cut. Here a cut in sphericity, $\ln(S) < -4.5$, has been used.

In two-jet events, the hadrons can also aquire p_{\perp} from soft gluons. The compensation of this p_{\perp} is in general not identical to the one assumed in the fragmentation, and depends on the recoil treatment of the cascade formalism. Thus the assumed p_{\perp} conservation length may depend on the treatment of recoils in the cascade, and on the cutoff scale, which determines to what extent hadron p_{\perp} originates from the cascade or the hadronization.

The top row in Table 2 shows results without cascade for the three different p_{\perp} correlation assumptions. Q_{\perp} clearly grows for less local p_{\perp} compensation, with a relative difference of 25% between complete p_{\perp} compensation by neighbours (JETSET default) and uncorrelated p_{\perp} . Adding a cascade allmost wipes out the difference, but after a two-jet cut it is restored to a satisfactory degree. The relative difference between the two extremes with a common cutoff $k_{\perp\text{cut}} = 0.6 \text{ GeV}$ (second and fourth column) is then about 16%. Also partial p_{\perp} correlation as assumed in [23], similar to the UCLA p_{\perp} generation model, gives results after a proper two-jet cut which differ significantly from the results of the JETSET default assumption.

A comparison of the first and second column illustrates the difference in p_{\perp} compensation in the cascade and in the fragmentation. The same p_{\perp} model, tuned with different cascade cut-offs, give significantly different results on Q_{\perp} . Soft gluon emission in the dipole cascade introduces longer p_{\perp} correlation lengths than given by default hadronization p_{\perp} , which implies that Q_{\perp} increases when adding soft gluons in the range 1.5 to 0.6 GeV to the cascade.

5.3 Screwiness

In [6], MC simulations of $q\bar{q}$ string fragmentation without cascade show a clear signal in $S(\omega)$ in the helix-like fragmentation model for $\tau \sim 0.5$ or larger. To check the influence of relatively soft gluons on the screwiness measure, we have modified JETSET to generate p_{\perp} according to the helix model. The p_{\perp} generation is then combined with the JETSET default recipe for passing gluons [20]. This implies that the azimuthal directions on different sides of a gluon kink is not completely uncorrelated, though measured w.r.t. two different directions. The p_{\perp} component being transverse to both considered directions is preserved when passing a gluon kink.

One could also consider more direct effects, assuming the azimuthal angle of vertices on different string segments to be explicitly uncorrelated, and also allowing the helix to have

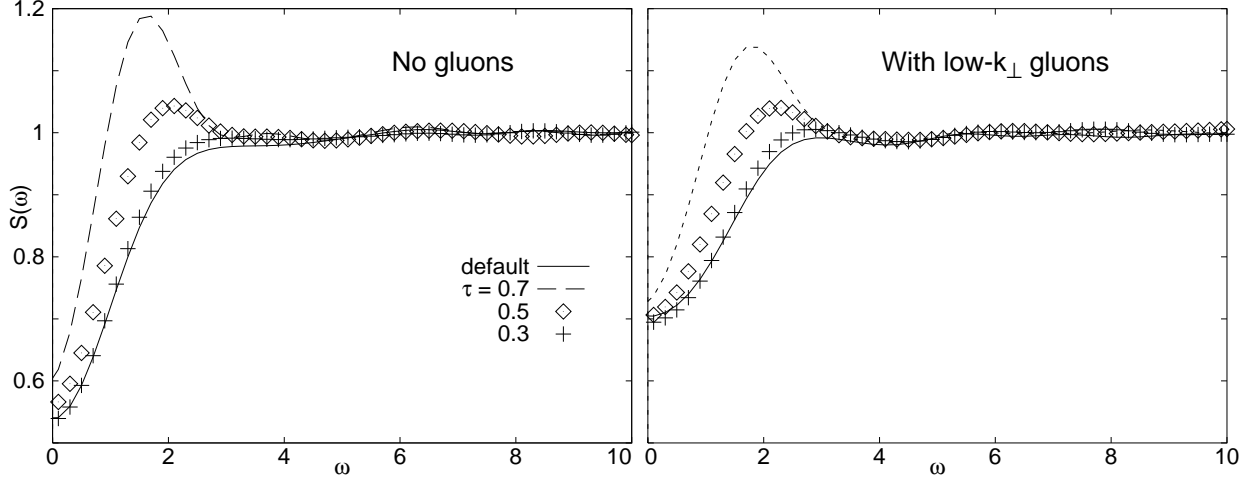


Figure 5: *Screwiness without gluons, and with low- k_{\perp} gluons (k_{\perp} in the emissions is restricted between 1 and 2 GeV). The central rapidity region $|y| < 2$ is considered. With the assumptions made here about effects from perturbative gluons, the signal survives.*

different orientation on different string segments. The investigation here however focus on the minimal effects of gluons bending the string.

Before looking at screwiness after a full cascade and a two-jet cut, we examine the effects of soft gluons by running a cascade with k_{\perp} for the emissions constrained between 1 and 2 GeV. As seen in Fig 5, the observable $S(\omega)$ is fairly unaffected by these rather soft gluons.

A cascade introduces long-range azimuthal correlations which have large effects on $S(\omega)$. In a three-jet event the thrust direction tends to be aligned with the hardest jet, which implies that the particles of this jet are rather randomly distributed in azimuthal angle ϕ . The softest jet is seen as a set of particles well collimated both in ϕ and y . The particles of the remaining jet are more spread out towards large rapidities and have an azimuthal direction opposite to the softest jet. In this typical three-jet configuration, particles of the hardest jet merely introduces noise to $S(\omega)$, while the two softer jets tend to enhance $S(\omega)$ when $\omega \sim \pi/y_{\text{cut}}$, where y_{cut} is the largest considered rapidity in the analysis. Thus we get a signal which is independent of fragmentation mechanism, but is sensitive to the magnitude of the considered central rapidity range. This behaviour is seen in the upper plots of Fig 6.

After event cuts (lower plots in Fig 6), the result is very similar to those with low- k_{\perp} gluons in Fig 5 and give a clear signal for helix-like string fragmentation if $\tau \sim 0.5$ or larger. In [6], different ways to enhance the signal also for lower values of τ were investigated. The analysis was performed on $q\bar{q}$ strings without cascade, and it was shown that a lower limit on average p_{\perp} could be used to distinguish default string fragmentation and helix fragmentation with τ down to 0.3. A lower cut in p_{\perp} is slightly in conflict with a two-jet cut, but it is possible that a similar approach can be used to enhance the signal in two-jet events obtained from real data.

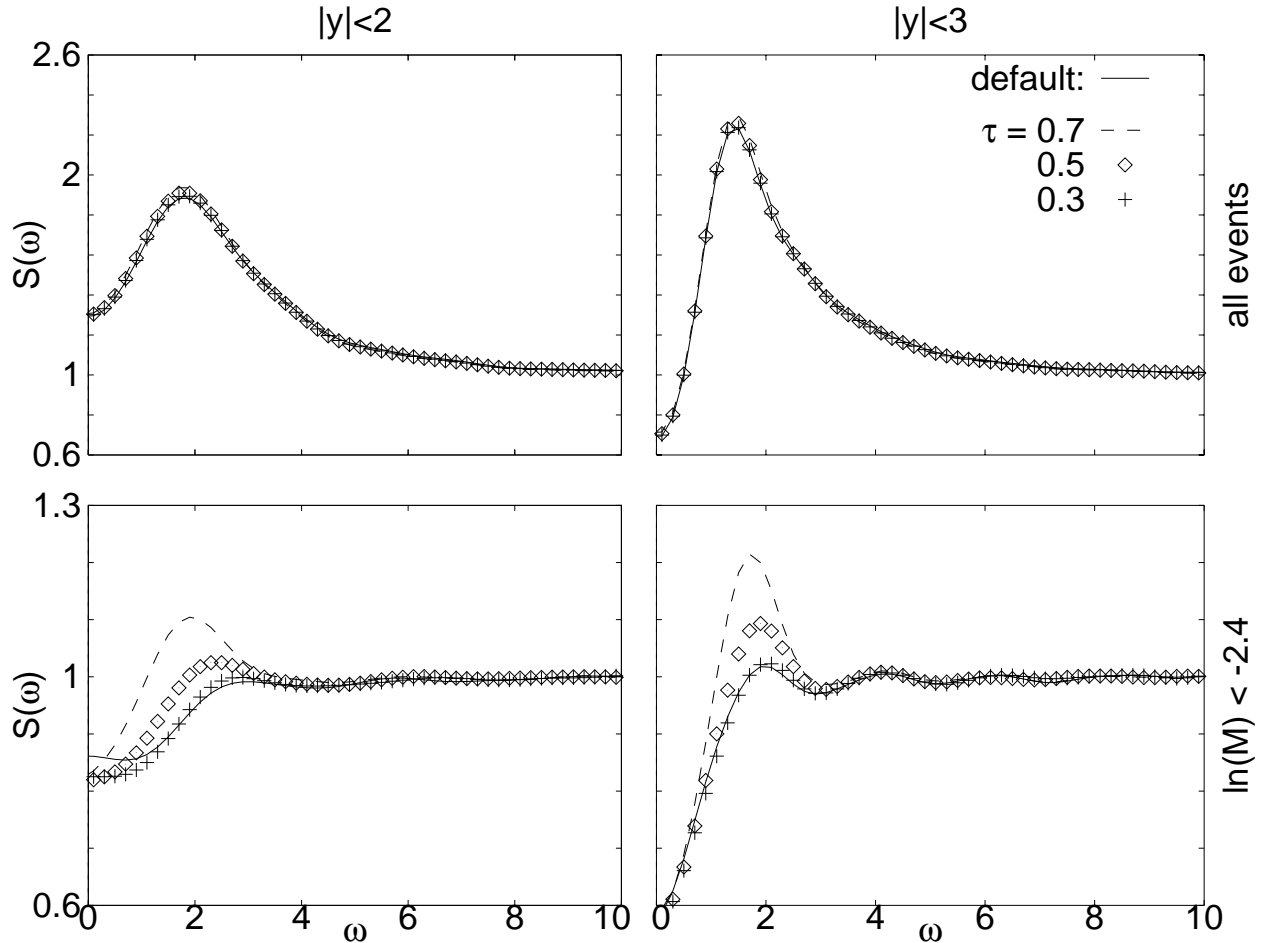


Figure 6: *Screwiness after gluon cascade, with and without a two-jet cut. Without any two-jet cuts (upper row), a signal reflecting long-range azimuthal correlations in three-jet structures is seen, independent of fragmentation mechanism. After a two-jet event cut, this signal is removed, and the $S(\omega)$ measure is sensitive to helix-like fragmentation. The results are similar to the ones with only low- k_{\perp} gluons, and only moderately reduced.*

6 Conclusions

High energy reactions like $e^+e^- \rightarrow \text{hadrons}$ are usually described in terms of two phases, an initial perturbative phase, formulated as a parton cascade, followed by a soft hadronization phase described by a phenomenological model. It is however not only the description of the soft phase which depends on model assumptions. This is also the case for the perturbative phase towards the end of the cascade, where α_s is large and some kind of cut-off is necessary. The transition region may also exhibit interesting interference or coherence effects, one example being the helix-like field configuration proposed in [6].

In many cases the effects of gluon emission overshadow the features of the hadronization phase. To investigate the hadronization mechanism it is therefore interesting to study whether suitable events cuts can help separating the two phases and give observables sensitive mainly to one of them.

We have examined different strong two-jet cuts to suppress the perturbative activity. It is possible to define efficiency and purity measures for the different cuts. MC simulations show, however, that no cut can be called optimal. Instead the preferred cut depends on the observable under investigation.

As the flavour composition of the final state in most models is less sensitive to the parton cascade, we concentrate here on observables related to transverse momentum. Different assumptions can be made concerning recoil effects and the locality of p_\perp conservation. In most models it is possible to tune the inclusive p_\perp spectrum, and to distinguish the models it is then necessary to study different forms of correlations. The vectorial sum of \mathbf{p}_\perp for all particles with rapidities smaller than some value y , here called \mathbf{Q}_\perp , is an observable which is sensitive to the p_\perp correlation length. If p_\perp is locally conserved, average Q_\perp is similar to average p_\perp . On the other hand, if only global constraints restrict p_\perp , the collective measure Q_\perp gets significantly larger than p_\perp .

After a two-jet cut, we find the Q_\perp measure to be sensitive to assumptions about p_\perp compensation in the hadronization phase. It is also sensitive to the value of the cascade cut-off, since the recoil treatment in the cascade in general give longer p_\perp correlation lengths than assumed in the fragmentation.

Another observable which is shown to be sensitive to the cascade cut-off is average p_\perp in low multiplicity events. Though multiplicity in general is not considered a two-jet cut, it suppresses high- k_\perp perturbative emissions, which typically give rise to large multiplicities. Gluon emissions with moderate k_\perp however contribute more to hadronic p_\perp than to hadronic multiplicity, which implies that the correlation between p_\perp and multiplicity is sensitive to the cascade cut-off.

In [6] it is argued that coherence effects in the transition region may give rise to a helix-like colour field, with a correlation between rapidity and azimuthal angle. Perturbative gluon emissions mask this correlation to a large extent, but we have found that after a strong two-jet cut, a signal in the proposed observable “screwiness” is present for some possible helix configurations.

The very high statistics now available from experiments at the Z^0 resonance implies that strong two-jet cuts are possible on the data without losing the statistical significance. Our results show that such cuts can indeed in many cases discriminate between different hadronization models and thus be a tool for a more detailed study of the hadronization mechanism.

References

- [1] D. Amati, R. Petronzio, G. Veneziano, *Nucl. Phys.* **B140** (1978) 54;
ibid. **B146** (1978) 29
- [2] Ya.I. Asimov, Yu.L. Dokshitser, V.A. Khoze, S.I. Troyan, *Z. Phys.* **C27** (1985) 65
- [3] B.R. Webber, *Nucl. Phys.* **B238** (1984) 492
- [4] C.D. Buchanan, S.B. Chun, *Phys. Rev. Lett.* **59** (1987) 1997;
C.D. Buchanan, S.B. Chun, *Phys. Rep.* **292** (1998) 239

- [5] B. Andersson, G. Gustafson, A. Nilsson, C. Sjögren, *Z. Phys.* **C49** (1991) 79
- [6] B. Andersson, G. Gustafson, J. Häkkinen, M. Rignér, P. Sutton, *JHEP* **09** (1998) 014
- [7] L. Lönnblad, *Comp. Phys. Comm.* **71** (1992) 15
- [8] M. Bengtsson, T. Sjöstrand, *Comp. Phys. Comm.* **39** (1986) 347;
T. Sjöstrand, *Comp. Phys. Comm.* **82** (1994) 74
- [9] G. Gustafson, *Phys. Lett.* **B175** (1986) 453;
G. Gustafson, U. Pettersson, *Nucl. Phys.* **B306** (1988) 746;
B. Andersson, G. Gustafson, L. Lönnblad, *Nucl. Phys.* **B339** (1990) 393
- [10] B. Andersson, G. Gustafson, G. Ingelman, T. Sjöstrand, *Phys. Rep.* **97** (1983) 31
- [11] L. Lönnblad, *Z. Phys.* **C58** (1993) 471
- [12] G. Parisi, *Phys. Lett.* **B74** (1978) 65;
J.F. Donoghue, F.E. Low, S.Y. Pi, *Phys. Rev.* **D20** (1979) 2759
- [13] W. Hofmann, *Ann. Rev. Nucl. Part. Sci.* **38** (1988) 279
- [14] L3 Collaboration, M. Acciarri et al., *Phys. Lett.* **B371** (1996) 126
- [15] E.A. de Wolf, private communications.
- [16] G. Marchesini, B.R. Webber, M.H. Seymour, G. Abbiendi, L. Stanco, I.G. Knowles,
Comp. Phys. Comm. **67** (1992) 465
- [17] B. Andersson, G. Gustafson, B. Söderberg, *Z. Phys.* **C20** (1983) 317
- [18] H. Bohr, H.B. Nielsen, *NBI-HE-78-3* (1978)
- [19] B. Andersson, G. Gustafson, T. Sjöstrand, *Z. Phys.* **C6** (1980) 235
- [20] T. Sjöstrand, *Nucl. Phys.* **B248** (1984) 469
- [21] ALEPH Collaboration, D. Buskulic et al., *Z. Phys.* **C57** (1993) 17;
L3 Collaboration, O. Adriani et al., *Phys. Lett.* **B292** (1992) 472
- [22] E.A. de Wolf, Contrib. to *Proc. XXII Symp. on Multiparticle Dynamics*, Santiago de Compostela 1992, ed. A. Pajares, World Scientific
- [23] B. Andersson, G. Gustafson, J. Samuelsson, *Z. Phys.* **C64** (1994) 653
- [24] N.K. Nielsen, *Nucl. Phys.* **B167** (1980) 249